INVESTIGATION OF A STRUT-BRACED WING CONFIGURATION FOR FUTURE COMMERCIAL TRANSPORT

G. Carrier, O. Atinault, S. Dequand, J.-L. Hantrais-Gervois, C. Liauzun, B. Paluch, A.-M. Rodde, C. Toussaint
Onera, the French Aerospace Lab; F-92190 Meudon, France

gerald.carrier@onera.fr, olivier.atinault@onera.fr, jean-luc.hantrais-gervois@onera.fr, anne-marie.rodde@onera.fr, bernard.paluch@onera.fr, clement.toussaint@onera.fr, cedric.liauzun@onera.fr, sylvie.dequand@onera.fr

Abstract

Strut-braced wing (SBW) is considered in the ongoing ONERA research project ALBATROS as one of a potential fuel-saving transport aircraft configuration. Although not a new concept [1] (several aircraft such as the Hurel-Dubois HD-34, 1956, have used this concept), it has recently received renewed interest since [2][3][4][5][6][7][8][9]. Indeed, the structural strut enables a reduction of the wing weight thanks to the reduction of the bending moment to be sustained by the wing box. The presence of the strut therefore enables to increase the wing aspect ratio, which results in direct aerodynamic performance gains, without considerable weight penalty as it is the case with conventional cantilever wings. The ALBATROS project aims at evaluating the potential of a strut-braced wing concept to improve the aero-structural efficiency of transonic transport aircraft. For that, specific studies are carried out to investigate the potential gains and possible problems of the concept in term of aerodynamics, structures and flight mechanics.

1. Introduction

Current societal and economical considerations/demands introduce new challenges for the civil aviation and commercial transport. Indeed, drastic improvements over current existing aircraft design in terms of energy efficiency, reduction of the environmental impact, increase of the passenger comfort and safety are expected, and ambitious targets to reduce energy consumption by nearly 70% over the next 30 years are discussed today. Incremental improvements of existing aircraft technologies while maintaining the aircraft architecture unchanged are not likely to allow reaching these ambitious targets; on the contrary, radical changes in the aircraft configurations will be required.

Among different candidate aircraft concepts being currently studied, the strut-braced wing (SBW) configuration has received much attention [8]. In year 2010, ONERA has launched an internal research project, named ALBATROS (Aile Laminaire hauBAnée à Traînée Réduite par Optimisation multidiSciplinaire), which is intended to evaluate and quantify the potential benefits of SBW aircraft and identify the possible showstoppers. This paper gives an overview of the work carried out at ONERA in the ALBATROS project.

The specifications and design hypothesis used to define a reference aircraft which is then used all along the project are introduced in the second section. This section also describes the preliminary design approach and tools used to define the ALBATROS reference design. The next section focuses on the aerodynamic design and evaluation studies. Then, the fourth and fifth sections present the structural design activities and the aeroelastic verifications

conducted on the reference configuration. Finally, the last section covers the flight mechanics and handling qualities considerations related to the high aspect ratio wing considered in this project.

2. Design specifications and preliminary design of the ALBATROS configuration

2.1. Methodology for configuration down-selection and preliminary design

The configuration was down selected using a method taught in the aircraft design course of the French engineering school ISAE-Supaero during the 1990's. This method presents a set of semi-empirical formulae convenient for designing a civil transport aircraft. Some formulae were modified in order to take into account the specific aspects of the configuration (such as laminar flow). The method relies on a classical future project approach, with iterative loops on weights and aircraft performance toward convergence on a mission objective (range and payload).

2.2. Design specification

2.2.1. Choosing a mission

Before iterating on main aircraft characteristics, the mission must be defined in terms of:
- payload (number of passengers);
- range;
- cruise speed;
- take-off field length (TOFL) and landing speed.

Other criteria such as noise, emissions, span limit can be included but are not main parameters for this study. The focus being on the pro and cons of a strut-braced wing, the purpose is not to assess for which aircraft such a solution is best suited, but to evaluate the benefit of this concept on a given type of aircraft. Two long-haul airliners being in development at the early stage of the project, a short-haul aircraft was chosen. Anyway conclusion can be extrapolated to other kind of aircraft thanks to the future project method.

The mission is supposed to meet given requirements from airline companies. We have chosen a mission that is typical of aircraft in the category of the A320 or B737, characterised by:
- 180 passengers;
- nominal range of 3000 NM, with daily mission of 500 NM;
- cruise speed at 0.75 Mach number, to take into account environmental stakes and to take benefit from laminar design on wing and strut;
- TOFL of 2,400 m and landing speed of 135 kts.

2.2.2. Freezing some parameters

Before defining a reference configuration, it is necessary to freeze some parameters:
- the configuration is designed with two turbofan engines on the rear fuselage in order to keep a wing as clean as possible;
- the wing being in top position, a T-tail is chosen;
- reference wing aspect ratio is fixed at 16, which is considered as the limit of what could be achievable without any strut (outcome of the NACRE EU project);
- wing sweep angle (at 25% of the chord) is frozen at 16° for laminar purpose.

2.2.3. Parametric study

A parametric study was first performed in order to choose a reference configuration in terms of:
- wing surface;
- engine sizing;
- flight level.

Main design objectives were fuel burn and direct operating cost (DOC), the later including trends in aerodynamics, weight and engine performance on an economic point of view.

For a given flight level, carpets containing the design objective (fuel burn or DOC) are plotted versus engine thrust and wing reference surface (see Figure 1). Red zones are not compliant with low speed requirements.
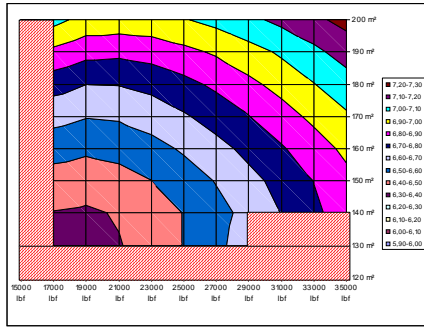
Figure 1. DOC carpet plot for an altitude of 39 kft

As a result, using similar carpet plots and fuel burn at other flight levels, the following aircraft parameters were chosen for the reference configuration:
- wing reference surface160 m²;
- engine thrust 22,000 lbf per engine;
- cruise altitude 39,000 ft.

This set of parameter provides a cruise CL of 0.59. Though not being the perfect optimum, this choice is a good compromise as a starting point for a reference configuration.

2.2.4. ALBATROS configuration design logics

Resorting to a strut-braced wing for this type of mission enables to implement several technological breakthroughs that can enhance the performance of such aircraft:

– the wing being supported by the strut, high aspect ratio can be used so as to limit the induced drag;

– the wing chord being modest, natural laminar flow can be enforced over most of the wing, thus reducing friction drag during cruise;

– thin profiles can be designed to gain on the profile drag and enable transonic operation with a moderately swept wing.

These technological choices infer a low sweep and therefore a relatively moderate Mach number (respectively 16° and 0.75 in this paper).

As for the aircraft architecture, the wing is necessarily in upper position to allow the strut to be in traction. In order to maximize the laminar flow, the motors are taken out of the wing and placed on the fuselage (aft position), leading to a T-tail.

2.3. Preliminary design approach and tools

Based on the design specifications, a rough aircraft can be designed. Semi-empirical formulas describing the aircraft design have been gathered into a python script that proceeds in the following manner:
1. definition of the fuselage dimensions (based on the number of passengers);
2. definition of the aircraft geometry (based on the wing main parameters);
3. estimation of the aerodynamic characteristics of the configuration;
4. estimation of the weight of the aircraft;
5. estimation of typical missions;
6. estimation of the global performance of the configuration.

Several iterations are carried out on the 4th step to achieve a coherent operating empty weight. Similarly, iterations are carried out on the 5th step to estimate the necessary fuel volume and weight. Globally, the succession of steps 4 and 5 is iteratively solved to converge on the empty aircraft weight and on the fuel volume.

These formulas derived from conventional aircraft are not well suited to the characteristics of the strut-braced wing (large aspect ratio, thin airfoil) and have been used to design a relevant aircraft without strut.

Nevertheless, the structural gains obtained thanks to the strut can be accounted for in the 4th step (beam models for the wing and the strut).

2.4. Description of the ALBATROS reference configuration

A reference configuration enabling to analyze the benefits of the strut-braced wing has been derived. The aim being to be able to compare to an equivalent conventional wing, the aspect ratio has been fixed to the limits of the conventional wings (16).

In the end, the preliminary design tool provides the general arrangement presented in Figure 2. The wing span is about 50 m for a fuselage length of about 41 m.
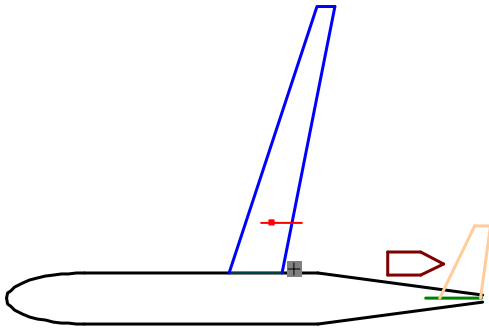
Figure 2. Preliminary design result.

Using the same general shape, the structural gains introduced by the strut are estimated. The resulting configuration does not reflect the complete benefit of the strut-braced concept, but it compares easily to conventional configurations (see Table 1). Despite the weight of the strut, the wing structure is alleviated and fuel is spared bringing an overall benefit for the companies by about 7%.

The wing laminarity is accounted for through an expected percentage of laminarity over the wing chord. 60% of laminarity (both upper and lower wing) has been inferred, leading to a gain in comparison to the turbulent wing by about 40 d.c., representing 14% of the total drag. The laminar wing allows reaching a complete aircraft drag of about 250 d.c..

	conventional	strut-braced
MTOW	85 t	78 t
Fuel weight	18 t	17 t
DOC	6.4 cent	5.9 cent

Table 1: Strut-braced concept overall gains.
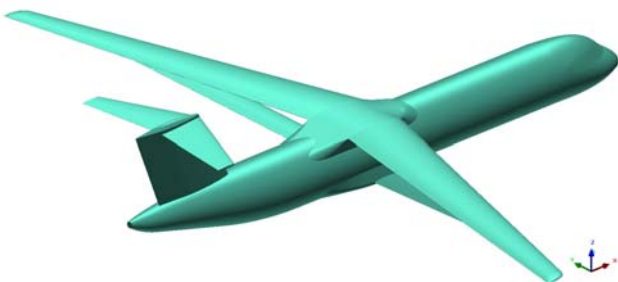
Figure 3. Generic view of the configuration.

3. Aerodynamic design activities

Following the preliminary design based on empirical formulations, it is important to analyze the configuration with higher order methods to determine precisely the benefits of the strut-braced configuration.

3.1. NLF wing design

From an aerodynamic point of view, the most important consequence of the strut-braced configuration is to increase the aspect ratio of the wing and therefore to decrease the induced drag. But, this concept also allows to minimize the relative thickness ratio of the airfoils and thus to reduce the wave drag and the pressure drag.

The choice of natural laminar flow which has been done has some effects not only on the airfoil definition but also on some parameters of the planform of the wing:

- the sweep angle at the leading edge should not exceed 18° to limit the transversal instabilities in the cruise conditions;
- the high taper ratio allows reducing the local Reynolds number at the wing tip and contributes to the laminarity.

These basic considerations have led to validate the main characteristics of the wing: the aspect ratio $\lambda = 16$, the taper ratio $\varepsilon = 0.35$, the sweep angle at 25% of the chord $\phi_{25} = 16^o$ ($\phi_{L.E.}=17.8^o$) and the relative thickness ratio of the airfoils between 6% and 10%.

3.1.1. Airfoils definition

To define the current airfoil of the preliminary wing, the 2D approach has been chosen (the high aspect ratio of the wing justifies the hypothesis of the oblique attack).

$M_{3D} = 0.75$ $\Rightarrow$ $M_{2D} = 0.721$
$C_{L3D} = 0.65$ $\Rightarrow$ $C_{L2D} \sim 0.7$
$Re_{3D} = 16.10^6$ $\Rightarrow$ $Re_{2D} = 15.10^6$

A 2D preliminary study in cruise conditions of the performance of natural laminar

airfoils with relative thickness ratios varying from 4% to12% leads to:

– rule out low thickness ratios airfoils. The balance between the drag gains and the drawbacks (mechanical resistance, small fuel volumes available, and low speed characteristics) is not good.

– eliminate the idea to have a proper behaviour at high-speed cruise conditions (M=0.79) with nominal cruise conditions at M=0.75 (too rapid increase of the pressure gradient on the upper side of the airfoil with the Mach number).

– choose only one airfoil to generate this laminar wing. The selected thickness ratio is nearly 10%.

The AO_01_10_C airfoil was defined with an inverse 2D method. The pressure gradient on the upper surface was chosen to provide a sufficient laminar flow part at a Mach number of 0.75 and a Reynolds number of 15.10^6 and to maintain a large enough leading edge radius to preserve the low speed performance.
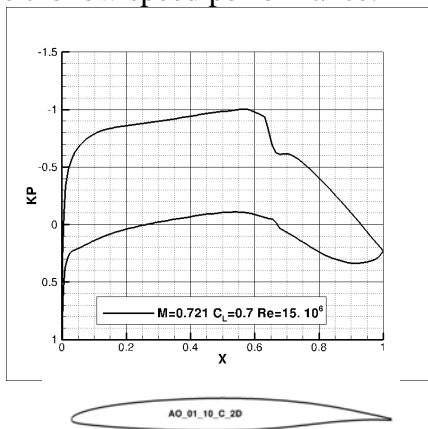
Figure 4. Pressure distribution on AO_01_10_C airfoil in cruise conditions.

The drag polars of the airfoil have been computed with the 2D coupled Euler+boundary layer code ISES in free transition at different Mach numbers show a laminar bracket around of the design C_L (0.7) until a Reynolds number of $30\ 10^6$. In cruise conditions the airfoil drag coefficient is 0.0033 and the transition is located near 60% chord on the upper and the lower sides of the airfoil.
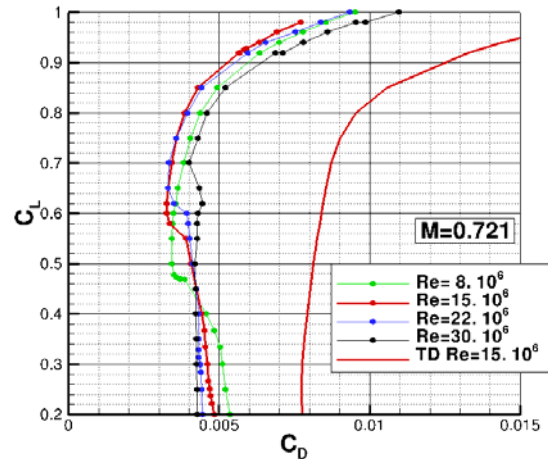
Figure 5. Free transition polars for various Reynolds numbers and fixed transition at Re=15 10^6.

In fixed transition, the drag coefficient increased more than 80%. The drag coefficient evolution versus the Mach number at C_L=0.7 shows a rather narrow bracket of very low drag around the cruise Mach number.
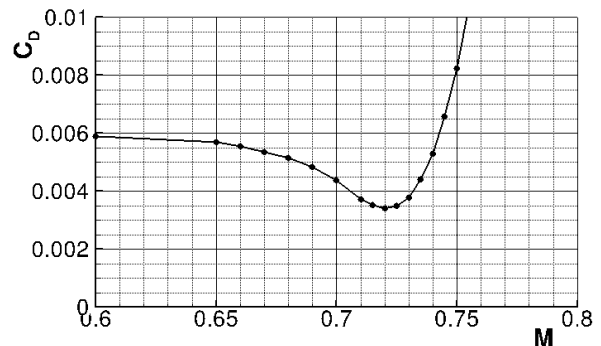
Figure 6. Drag coefficient evolution versus Mach number (2D Mach number).

3.1.2. Preliminary evaluation of the wing

This unique airfoil was used to generate a former wing with geometrical characteristics listed below. The wing performances have been evaluated with a potential method with a strong coupling of a 3D boundary layer.

Sref	160 m^2
Aspect ratio	16
Sweep 25%	16°
Span	50.60 m
Chord root/tip	4.496/1.574 m
m.a.c.	3.269 m
Thickness ratio	10%

In spite of the addition of a twist law to limit the flow acceleration at the root and the tip of the wing, it was necessary to adapt the airfoil at the root to reduce the intensity of the pressure recovery. A modified airfoil, adapted to the root conditions, was deduced from the current airfoil by moving forwards the location of the maximal thickness.

The calculation of this new geometry in cruise conditions shows therefore a rather good regularity of the pressure gradients along the span and a natural laminar flow over 35% on the upper side of the wind and over 40% on the lower side (Figure 6).
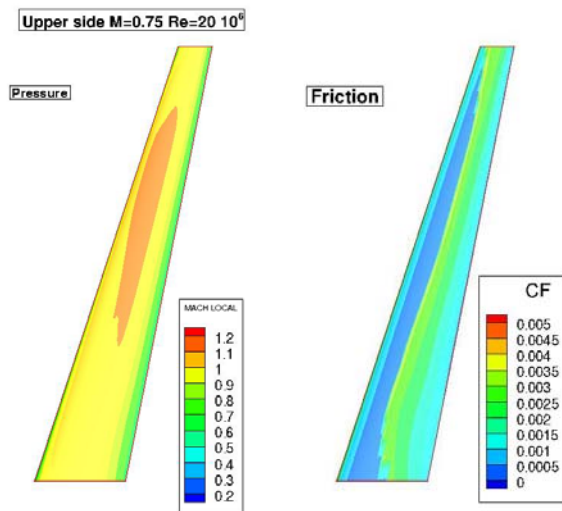
Figure 7. Local Mach number and drag coefficient on the upper side of the wing.

3.1.3. RANS assessment

Based on previous design with a single profile over the complete wing span (with only a modification at the root), a CAD model for the wing alone has been derived using CATIA V5. A Küchemann wing tip has been added and a RANS mesh has been made using ICEM HEXA. RANS simulations with the elsA[4] software have been carried out on the wing alone to establish the behavior of the NLF wing. The natural transition is modeled within the elsA software and both transverse and crossflow transition criteria are accounted for.

The twist has been adapted so as to reach a low drag at cruise. As the wing is not subjected to wave drag, an elliptic loading is adequate.

This loading has been adapted to enable a large portion of the wing to work at the local lift coefficient where the profile produces its best results (see Figure 8).
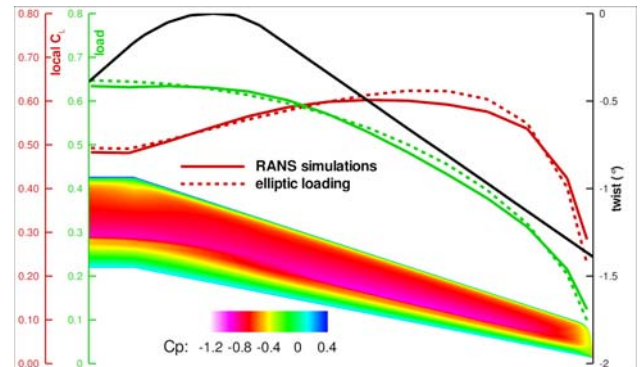
Figure 8. Loading of the laminar wing.

The upper wing surface exhibits a laminar behavior up to the shock recompression (two thirds of the chords) and about the third of the wing chord on the lower wing (see Figure 9). The laminar behavior is preserved across the lift polar providing about 30 d.c. gains in comparison with the completely turbulent wing. This is to be compared with the 120 d.c. at cruise for the laminar wing.

This extension of laminarity and the associated drag gains (30 d.c.) are consistent with the percentage estimated at the pre-design stage (40 d.c.), even though the laminar zone extent is somewhat lower over the lower wing surface.

Apart from the cruise behavior, no heavy flow separation is encountered up to M = 0.78 and C_L = 0.80 and no drag divergence issues occur (margins by 0.01 in Mach number and 0.10 in lift about the cruise).
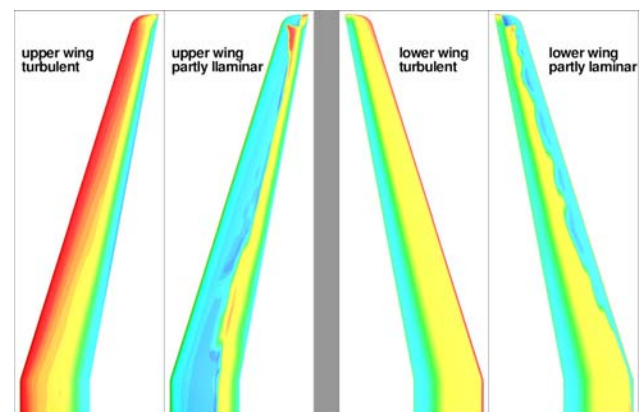
Figure 9. Local friction coefficient.

3.2. 3D wing-body design

Body alone drag polars have been established in order to define the correct setting of the wing on the fuselage for a cruise at the most favorable incidence. Then, a detailed design of the wing fairing on the fuselage has been carried out with the CATIA V5 software (see Figure 10). In this study, the aim is not to define an optimized fairing but to derive a realistic junction enabling to assess globally the aerodynamic performance of the glider.

The behavior of this design has been analyzed numerically to check the absence of any flow separation (see Figure 11).
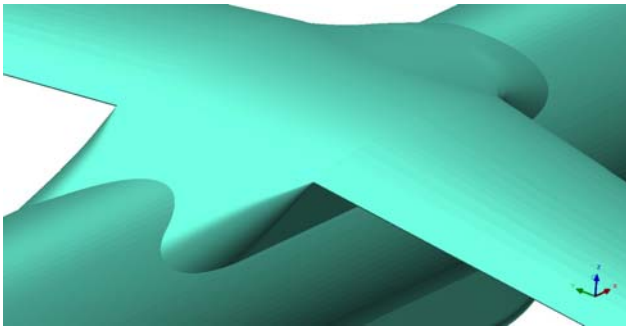
Figure 10. CAD of the wing – body junction.
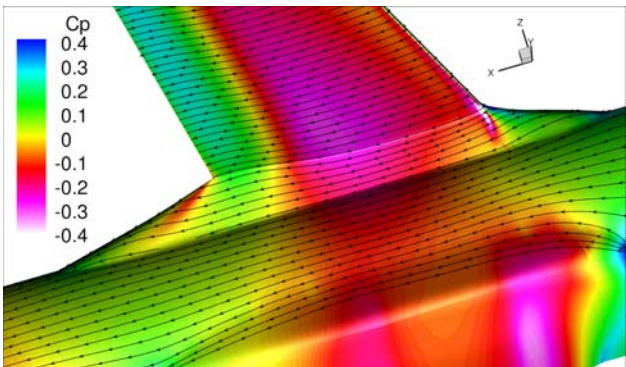
Figure 11. Aerodynamic behavior of the wing – body junction.

3.3. Aerodynamic evaluation of first design variants

Preliminary computations have been carried out on the configuration (no strut). An effect of wing sweep has been estimated (change by 2° of the wing sweep, see Figure 13). The effect over the lift over drag ratio is illustrated in Figure 13.

The design variants topic will be continued further.
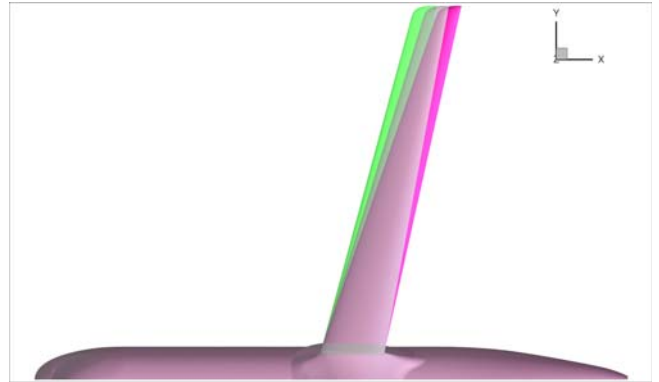
Figure 12. Wing sweep effect (the colored shapes have plus or minus 2° in sweep in comparison with the reference gray shape).
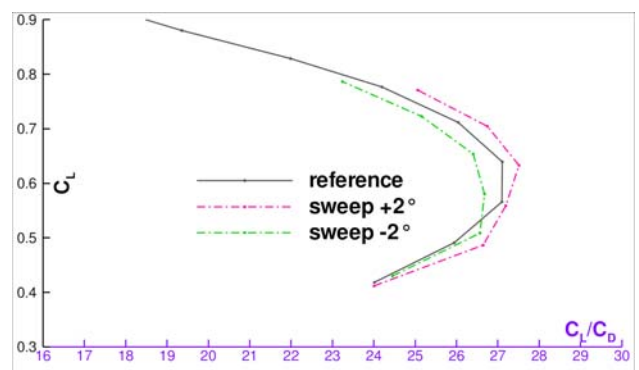
Figure 13. Lift over drag ratio for different wing sweeps (turbulent mode).

4. Structural design

4.1. Foreword

The main goal is to determine the weight saving due to a strut-braced wing. The primary structure of this wing remains unchanged compared to a classic one, but the use of small relative thickness (10 % or less) laminar airfoils imposes to use a strut to improve the lack of wing's flexural stiffness. To estimate the weight of this structure, it is necessary to size the following components: the upper and lower skins supporting the compression and tensile stresses induced by wing deflexion, the stiffeners laid out on the skin inner sides in the wing span direction to avoid the local buckling phenomena between two consecutive ribs, the spars which support the shearing forces, and the ribs. The devices fixed on the leading (slats) and trailing (flaps, ailerons) edges are considered as

secondary structures, so their weights are estimated through statistical formula.

4.2. Materials

The current trend is to use extensively thermoset resins with carbon fibre reinforced composite materials in the next generation of aircraft wings. In order to reduce the manufacturing costs, two kinds of complementary Liquid Composite Moulding (LCM) processes can be used to replace partially prepregs: the Resin Moulding Transfer (RTM) or the Vacuum Assisted Resin Moulding Transfer (VARMT). A combination could be used to reach this goal, such as prepreg automatic layer taping for the skins, with higher mechanical properties, and LCM for more complex parts such as stiffeners, spars or ribs. *Table 1* gives an example of elastic properties of unidirectional carbon/epoxy which can be obtained at an industrial scale, and taken into account to perform the weight estimation.

Property		Prepreg	LCM
E_1	GPa	130,0	120,0
E_2	GPa	9,8	9,0
G_{12}	GPa	4,4	3,8
ρ	kg/m^3	1 560	1 520

Table 1: comparison of main elastic properties of carbon/epoxy prepreg and LCM.

Regarding the stacking sequences, several strategies can be adopted. The use of conventional ply angles, instead of optimised ones allow to save a large amount of computing time. Consequently, only laminates made up of 0° (l %), 90° (m %), +45° (n_1 %) and -45° (n_2 %) plies (angles are defined according to the wing span direction x, figure 15) had been used, with: $l+m+n_1+n_2=100\%$. These proportions have to satisfy some rules, well established now [5]. The following values of allowable strains were taken into account: $\varepsilon \leq 0,5$ % for the limit loads, and for $\varepsilon \leq 0,3$ % the ultimate loads. The first value includes a reduction factor due to the material fatigue and damage tolerance. The stacking sequences have to be symmetrical to minimize the curing residual strains but, if (l, m, n_1, n_2) are even, the choice of laminate thicknesses is drastically limited. By relaxing slightly this condition we are able to build a

larger family of laminates (Figure 14) which leaves more freedom in optimal thickness research.
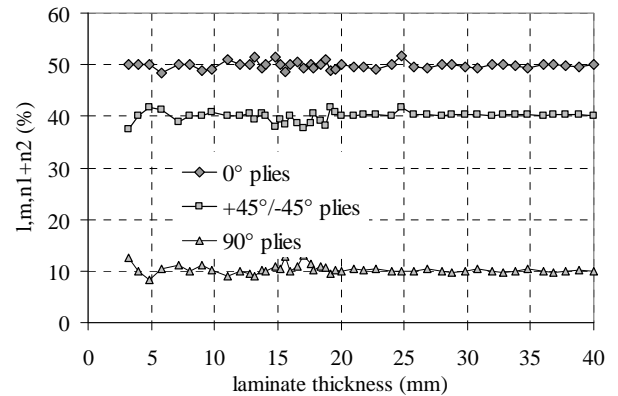
Figure 14. Extended family of allowable laminated.

The use of composite materials, compared to aluminum alloys, is very attractive in terms of weight saving. However, their low electrical and thermal conductivities rise two types of problems: lightning resistance and electromagnetic compatibility. The most traditional solution consists in inserting copper cloths between laminate plies and to use metal deposit (on rib, spar and stiffener external sides) to ensure the electric connections between the various wing components. These additional masses are included in the final weight breakdown.

4.3. Buckling

The elastic stability of the skins is ensured by the ribs and the stiffeners. Very close ribs should avoid stiffeners, but lead to heavy wing and higher manufacturing costs. In this work a typical rib spacing varying from 0.4 to 0.7 m is considered, according to some authors recommendations [7]. To determine the optimal size of the stiffeners and their spacing, several approaches are possible. An analytical formulation based on the classical theory of plate elastic stability has been used [6], in which the wing box shape comprised between two consecutive ribs is simplified by a rectangular box, subjected to a bending moment M_b, which dimensions are L_c, H_c and B_c (from step a to step c, figure 15). Upper and lower skins are then considered as simply supported panels subjected to a uniform compression force F_c (step d, figure 15).
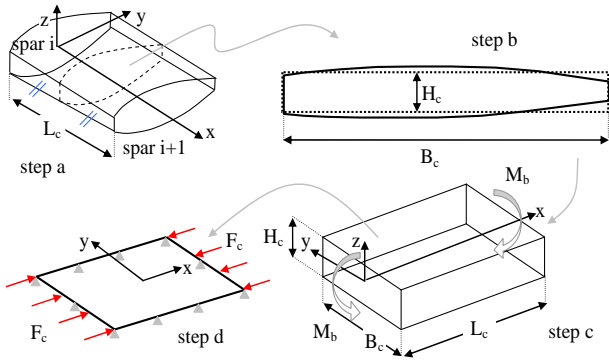
Figure 15. Simplified wing box geometry.

Among the most usual stiffener cross sections (Z, J and Ω), we used the J shape due to his higher inertia/mass ratio. For the stiffeners, the number of parameters to optimize is focused on two variables: e_L and b_L (Figure 16). Other dimensions are function of b_L, with the following ratio $k_h=h_L/b_L$ and $k_a=a_L/b_L$ respectively equal to 1.2/0.4 (usual values). The method of optimization consists in seeking the solution which simultaneously satisfies the preceding allowable strain criterion (to find e_S) as well as the non buckling condition, while minimizing the mass of the skin and stiffener set. An additional constraint concerns the minimal allowable distance between stiffeners (D_L) to avoid higher manufacturing costs.
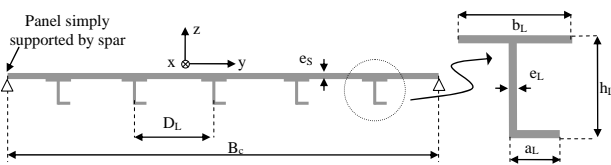
Figure 16. Dimensions of a stiffened skin considered as a simply supported panel.

Figure 17 illustrates the results obtained for a 10 % laminar airfoil, with a chord of 4 m, L_c=0.5 m and a bending moment of 900 kNm. B_c is equal to 2.4 m and H_c to 0.34 m. The skin thickness e_S is equal 7.2 mm, with 9 stiffeners (b_c=52 mm, e_L=7.75 mm) and D_L=0.24 m (the stiffeners had been repositioned on the real airfoil). In main cases, only few iterations are necessary to find an accurate solution.
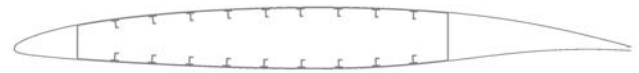
Figure 17. Example of optimized wing box obtained on laminar airfoil.

4.4.   Loads

Only the aerodynamic lifting loads are taken into account, with positive (case A, f_L=2,5 g) and negative (case B, f_L=-1g) load factors f_L. Since the strut airfoil is symmetric, we assumed that it does not support any lifting force. The lifting loads had been calculated according to an elliptic distribution, and Figure 18 illustrates such a distribution for a MTOW of 82 t.
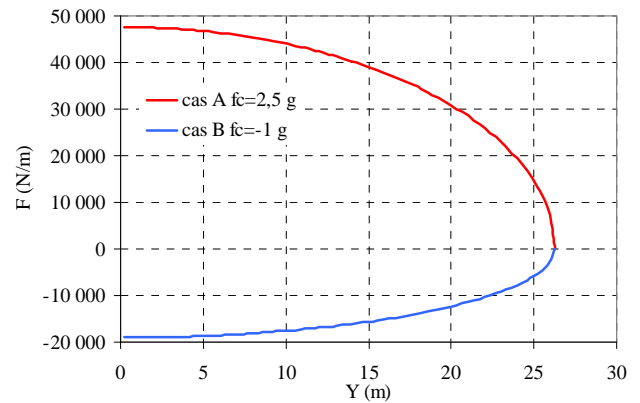
Figure 18. Example of lifting load distributions calculated for cases A and B (MTOW = 82 t).

The third case (C) concerns the loads which can occur in case of "hard" landing. Standards as well as the maximum vertical speed allowable lead to the following assumptions: maximum vertical acceleration of 2g, wing full of fuel, and no lifting force.

4.5.   Wing sizing procedure

The simplified wing calculation model is composed of three distinct parts (Figure 19): the central wing box (A), the strut (B) and the mast (C). Due to their high aspect ratio all these parts are considered as beams. In addition to the wing geometry the other main geometrical parameters which influence the wing weight are L_h, Z_h and D_a. The ideal case leads to highest and lowest values of Z_h and D_a respectively, in order to limit the upward wing deflection. Z_h is limited by the height of the fuselage, ie 4 m in this work. However D_a cannot be null for

aerodynamic considerations, D_a=0.2 m seems to be a good compromise.
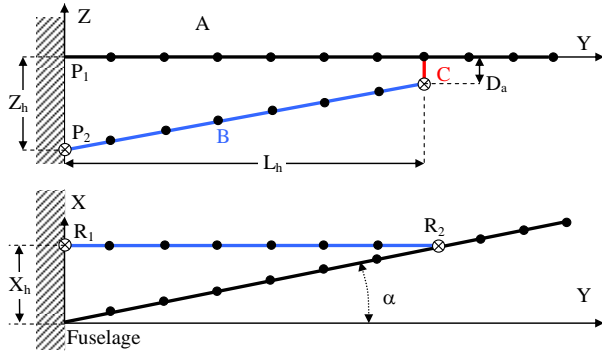
Figure 19. Wing finite beam element model.

To minimize the weight of the strut, it only has to support tensile or compression forces, so two pinned joins (R_1 and R_2, Figure 19), are located at its ends. Since the structure is not isostatic, a finite element method [[14]] is used, with linear interpolation beam elements and 6 degrees of freedom per node. The forces taken into account for the three loading cases are aerodynamic (case A and B), inertial, and gravity loads. Each wing element has the length of the wing box comprised between two consecutive ribs (figure 20). The mast (C) is meshed with only one element, while the strut (B) is meshed with approximately 0.5 m length element. The whole model is composed of about hundred elements, which allow calculating (in the centre of each element) the bending curvatures and, consequently the moments acting on wing boxes, with good accuracy. The calculation procedure is iterative, with the following steps:

a) calculation of rib spacing according to the local airfoil wing thickness, and meshing with beam elements;

b) determination of skin thicknesses and stiffener size for each wing box (e_S, e_L, b_L and D_L) e_L and e_S being chosen among the laminate family (Figure 14);

c) calculation of the element stiffnesses (EI, GJ,…);

d) calculation of node displacements for all loading cases, maximum bending moments M_b at each element centre is then deduced from strain and curvature interpolation;

e) return to step b) if one of the element does not respect sizing rules.

In order to accelerate the convergence, the initial bending moment distribution along the wing span is calculated with strength simple analytical formulas. Although the values are not exact, this distribution is a good starting point allowing great time saving, particularly in a future Multi Disciplinary Optimization (MDO) approach. In most cases less than 5 or 6 iterations are necessary to find a solution. Figure 20 shows views of rib spacing and skin thickness laminate calculated with the previous calculation procedure.
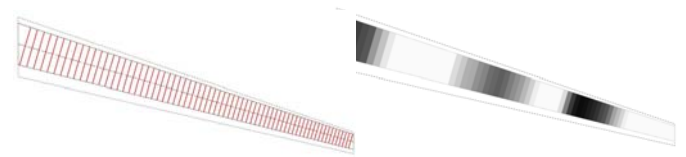
Figure 20. Typical rib spacing (left) and skin thickness variation (right) along span obtained for a strut-braced wing.

4.6. Structural sizing results

Figure 21 shows the variation of the W/W_{min} ratio, W_{min} being the minimal weight of the wing (about 2950 kg for a half wing), according to the wing span ratio X. For a strut located between 50 and 70 % in span, the wing weight is very close to the minimum value (W does not exceed 5% of W_{min}). Below 50% the strut is more and more ineffective and beyond 70% its weight becomes too important.
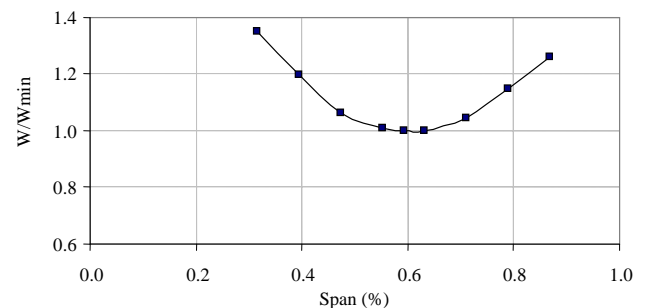
Figure 21. Plot of the ratio W/Wmin vs wing span ratio X.

The calculations obtained with the previous FE beam model were checked with a more refined FE model composed of plate elements (Figure 22). This model confirms the accuracy of the beam FE model assumptions, and showed the interest to use a curved strut.

When the wing bends upwards (case A), the strut becomes straight. When the wing bends downwards (case B), the strut buckles down, without risk of touching the lower wing skin, (such situation could occur with a rectilinear strut). In addition, strut buckling enables it to support important displacements with moderate strains. That will avoid the use of expensive and heavy mechanical devices located in the fuselage (at R_1, Figure 19) to relieve the strut from the compressive forces.
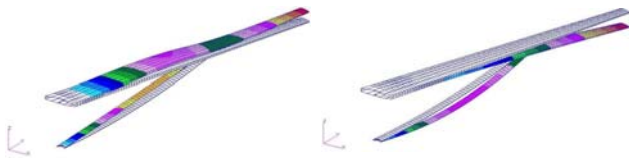
Figure 22. Typical wing deflexions calculated with a detailed FE model (left : case A, right : case C). Coloured surfaces show the deformed structure.

For the same wing geometry, calculated without strut and with thicker airfoils at wing root, the estimated weight is about 5200 kg (for a half wing), so weight saving due to a SBW wing is about 40 %.

5. First aeroelastic evaluations

This section deals with the aeroelastic analysis of the SBW concept, in order to evaluate its aeroelastic stability.

5.1. Original configuration

An aeroelastic analysis was first performed on an original configuration with a straight strut located at a wing span ratio of 71% (model 1 in Table 2).

In a first step, the structural modes of the SBW configuration are determined by performing a modal analysis using the MSC software Nastran [15]. This modal analysis is performed using clamped wing-root boundary conditions and pivot boundary conditions for the strut. The aeroelastic study, carried out with the in-house numerical tool "CAPRI", is then limited to the first 40 modes of the structural model, with modal frequencies between 1.23Hz and 99 Hz; and only symmetric modes are taken into account. Using the infinite plate method,

these structural modes are then projected onto an aerodynamic mesh composed of two planes, with respectively 1472 and 262 quad elements, modelling the wing and the strut (Figure 23Figure 24). The aerodynamic forces can then be computed using the Doublet Lattice Method (DLM) [16], based on the linear aerodynamic potential theory. Finally, the flutter equation is solved using the P-K method (or double scanning method) [17][18], for Mach numbers ranging from 0.3 and 0.82.
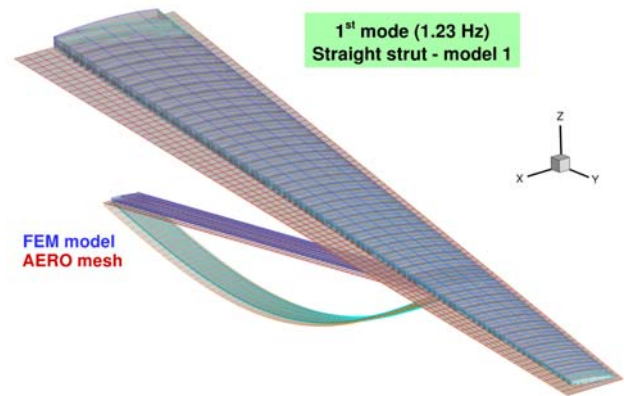
Figure 23. Visualization of the 1st flexion (1st mode) of the strut (model 1 in Table 2.).

The results of the flutter analysis show the evolution of the aeroelastic frequencies and damping coefficients in terms of the altitude. As shown in Figure 23, the damping coefficients of the first five modes remain positive and no flutter phenomenon is detected for the SBW configuration. This is also verified for the other modes.
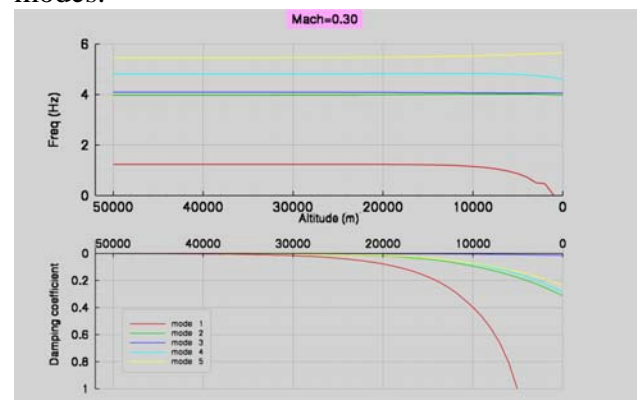
Figure 24. Model 1 - Flutter curves for modes 1 to 5 at Mach=0.3.

However, the first mode of the SBW configuration has a behaviour which is typical of a static divergence, with a frequency tending

towards zero and a damping coefficient becoming infinite. This first mode corresponds to the first flexion of the strut (Figure 23Figure 24) and the reasons of its static divergence in the flight domain are still under investigation.

As a static divergence is generally due to the torsion of the structure, another flutter analysis has then been performed on a modified structural model, in which the thickness of the strut skin was multiplied by two (model 2 in Table 2.). When the strut stiffness increases, the critical altitude at which the static divergence occurs is indeed shifted towards lower values. Hence, doubling the skin thickness of the strut enables to shift the critical values out of the flight domain for low Mach numbers, but is however not sufficient for higher Mach numbers (Figure 25).

An update of the strut design is therefore necessary in order to avoid the appearance of this static divergence phenomenon.
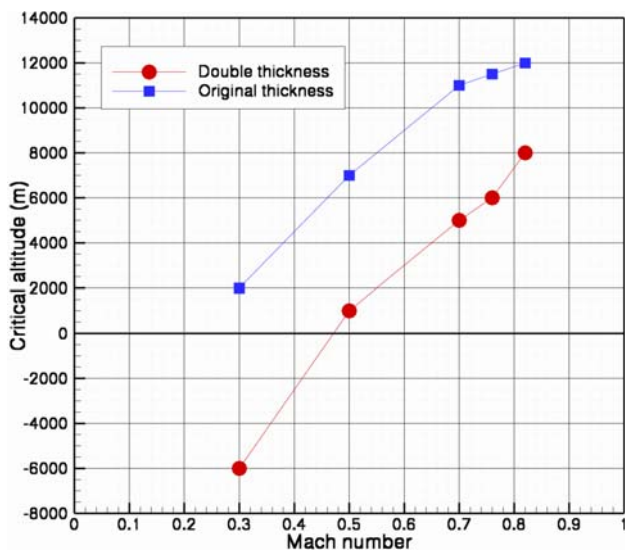
Figure 25. Critical altitudes, at which the static divergence occurs, as a function of the Mach number. Comparison between the original (model 1) and the modified strut (model 2).

5.2. Parametrical study

In order to identify which parameters are important for updating the strut design, several configurations have then been studied. The parameters considered are:
- the curvature ratio of the strut (0%, 5% and 9.5%);

- the position of the strut relatively to the wing : wing chord ratio and wing span ratio;
- the thickness of the strut elements.

Table 2. gives a list of the different configurations tested.

Model nb.	Strut curvature ratio (%)	Wing chord ratio (%) (strut X-position)	Wing span ratio (%) (strut Y-position)	Strut thickness (m)
1	0	50	71	0.0071
2	0	50	71	0.0142
3	0	50	59	0.0071
4	5	50	59	0.0071
5	9.5	50	59	0.0071
6	0	20	59	0.0071
7	5	20	59	0.0071
8	5	20	59	0.0142
9	5	20	59	0.0213

Table 2. List of the models with their characteristics.

When the strut is curved (models 4, 5 and 7 to 9), the 1st mode corresponds to the flexion 1 of the wing (Figure 26) and the strut mode, for which static divergence occurred (for the straight strut), does not exist anymore. However, a static divergence of this 1st mode still appears.
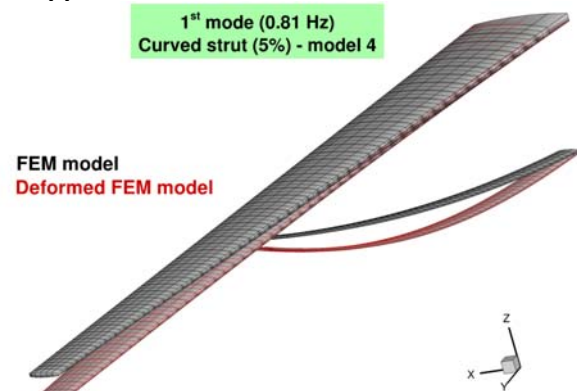
Figure 26. Visualization of the 1st flexion (1st mode) of the wing (model 4 in Table 2.).

Figure 27 shows the critical altitudes obtained for the different models, at given Mach numbers ranging from 0.3 to 0.82. According to the configuration studied, these critical altitudes correspond either to the altitude at which a static divergence or a flutter instability occurs.
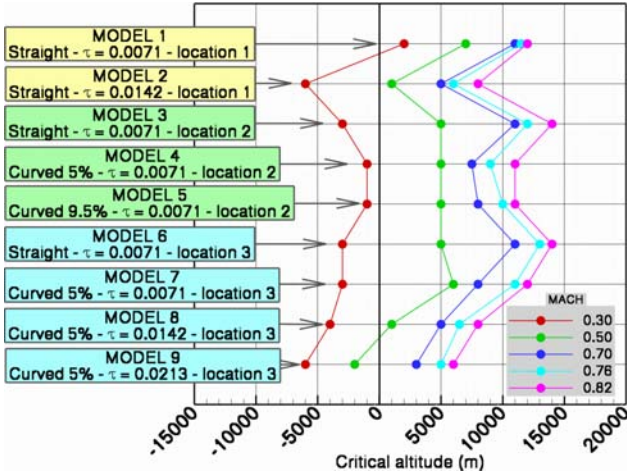
Figure 27. Critical altitudes of the 9 different models studied (Table 2). Each curve corresponds to a given Mach number.

From the different tests performed, one can conclude that:

- the position of the strut relatively to the wing does not have a significant effect on the aeroelastic stability of the concept;
- considering a curved rather than a straight strut will have a significant effect only for high Mach numbers (comparison between models 3 and 4, or 7 and 8, in Figure 27); however, the decrease of the critical altitude is not sufficient to guarantee the aeroelastic stability;
- increasing the thickness of the strut improves the aeroelastic behavior of the concept: when the thickness of the strut structure is increased by a factor three (model 9), no aeroelastic instability occurs in the flight domain.

The first aeroelastic analyses performed on the SBW concept show instabilities (static divergence and flutter) in the flight domain. From the few preliminary tests carried out in order to improve the aeroelastic stability, it results that the most significant effect is obtained when increasing the thickness of the strut. Further tests are still under investigation (such as the introduction of punctual masses, or located thickness changes on the strut). However, it is already clear that an update of the strut design will be needed.

6. Handling qualities considerations

High aspect ratios made possible by the SBW configuration are advantageous for aerodynamics, but may turn out troublesome as regards handling qualities, more specifically for performing roll maneuvers. This question has to be addressed soon in the design process since it may impact not only the control surface sizing, but the very efficiency of the classical roll devices, i.e. ailerons.

Airworthiness regulations [19][20][21] define minimum roll performances in terms of bank angles that must be reached within given time lapses. More simply, in the preliminary design phase only the achievable roll rate is considered, as this is the main contributor to the ability to pass the roll maneuvers.

The question addressed here is to assess the impact of high aspect ratios on the roll rate: how does it vary with the design variables; and does aileron efficiency remain sufficient?

The achieved roll rate results from the equilibrium between the roll momentum due to ailerons, and the aircraft roll damping, mostly due to the wing. In a flexible aircraft both aerodynamics and structure contribute to those momentums. However, flexibility is not taken into account in this first assessment, because 1/ the SBW configuration is meant not to be flexible; 2/ consequently, critical roll rates are expected at low speeds where flexible effects are the lowest. Therefore the proposed study relies solely on aerodynamics.

Using the strip theory, the roll momentums are obtained by integrating along the span the lift on each wing section, multiplied by the lever arm. It is convenient to take all the dimensioning terms out of the integral, leaving only a dimensionless integral. The roll momentums due to the ailerons deflection δl, $L_{\delta l}$, and to the roll rate p, L_p, can thus be written:

$$L_{\delta l} = \overline{q} c_m b^2 k_{\delta l} \delta l \quad \& \quad L_p = \overline{q} c_m b^2 k_p \frac{pb}{V} \qquad (1)$$

where $k_{\delta l}$ and k_p are the dimensionless integral terms developed below, $\overline{q}$ the dynamic

pressure, b the wing span, c_m the mean aerodynamic chord and V the airspeed.

$$k_{\delta l} = \int_0^1 \frac{c(\eta)}{2c_m} C_{L\delta l}(\eta)\eta \, d\eta \qquad (2)$$

$$k_p = \int_0^1 \frac{c(\eta)}{2c_m} C_{L\alpha}(\eta)\eta^2 \, d\eta \qquad (3)$$

η being the reduced abscissa along span, $c(\eta)$ the local chord, $C_{L\alpha}$ and $C_{L\delta l}$ the local lift gradients wrt to a.o.a., α, and aileron deflection.

The dimensionless expressions have a major interest: they only depend on the wing shape and aileron placement relative to the wing, not on the sizes, and this dependency is limited: a rough estimate is easily available in preliminary design. If the aspect ratio λ is increased while keeping the other parameters (chord distribution, sweep angle and aileron placement), $k_{\delta l}$ and k_p will be increased by a few percent following the aircraft lift gradient, but their ratio will remain almost unchanged.

Balancing the roll momentums yields a simple expression of the achieved roll rate.

$$p = -\frac{k_{\delta l}}{k_p} \frac{V}{b} \delta l \qquad (4)$$

The roll rate is proportional to V, and inversely proportional to the span b. As expected, increased span leads to decreased roll rate for the same aileron position (relative to span and chord) and deflection. But the drivers are V and b, not directly the aspect ratio. Since the aimed configuration aims typical transport aircraft minimum speed, and that the span resulting from increased aspect ratio is not uncommon (lower than an A330's), it can be concluded safely that classical roll devices, such as A330's or A380's, will be sufficient to give the studied aircraft the needed roll performance.

The V/b ratio may be related to design parameters by applying the lift equation:

$$\frac{V}{b} \propto \left(\frac{m}{S}\right) \frac{1}{\sqrt{m}} \frac{1}{\sqrt{\lambda}} \qquad (5)$$

Further than the strip theory analysis, numerical validations based on Vortex Lattice Methods have been conducted in order to assess with better accuracy both the aileron roll efficiency and the wing roll damping with respect to aspect ratio.

7. Future work

This research activity conducted within the ONERA project ALBATROS will be continued until 2013 and several complementary tasks will be performed. After the definition of the reference ALBATROS configuration, the aerodynamic evaluation and design activity will focus on the evaluation of several design derivatives. The impact on the aerodynamic performance of the aircraft of several parameters such as the aspect ratio, the sweep angle, wing thickness and strut/wing junction position and shape will be investigated.

In term of structures, the efforts will be put on the investigation of the aeroelastic phenomena occurring on the reference configuration and on selected design derivatives.

Finally, based on the different tools developed and calibrated in these disciplinary studies, a MultiDisciplinary Optimization (MDO) system will be put in place and applied to investigate more thoroughly the design space defining the strut-braced wing configuration. This shall help to identify the best compromise and balance between the aerodynamic and structural benefits of the concept that can be exploited to optimize the overall aircraft performance for the target mission.

8. Conclusion

This paper gives an overview of the research activities conducted by ONERA in the ALBATROS project on a strut-braced wing (SBW) transport aircraft configuration. This project focuses on the aerodynamic and structural design of a SBW transonic transport aircraft. The aim of this project is to evaluate the potential gains in term of aerodynamic efficiency and structural weight offered by the SBW concept and to identify the possible difficulties associated to such type of configuration.

In this context, the SBW concept is utilized to increase significantly the wing aspect ratio, reduce the wing sweep angle and profile thickness in order to achieve laminar flow on a large part of the wing surface. Compared to conventional commercial aircraft cantilever wing, these wing characteristics enable remarkable aerodynamic efficiency improvements which have been evaluated by RANS CFD calculations.

In term of structural design, the SBW allows to keep a relatively light wing primary structure despite the significant aspect ratio increase and the limited wing box thickness. A dedicated FE-based sizing software has been developed to design the wing+strut structural assembly. Furthermore, aeroelastic analyses are under progress in order to check that the SBW does not exhibit unacceptable dynamic behaviors.

The impact of the high aspect ratio wing on the aircraft handling qualities is also considered in the project, and the last task will consist in applying a MDO approach to identify the maximum overall aircraft performance gains achievable with the SBW configuration.

9. References

[1] M. Hurel, "The Advantages of High Aspect Ratios," Interavia, Volume VII, No. 12, 1952, pp. 695-699

[2] Amir H. Naghshineh-Pour, "Structural Optimization and Design of a Strut-Braced Wing Aircraft", Master of Science Thesis submitted to the Faculty of the Virginia Polytechnic Institute and State University, November 30, 1998

[3] F. H. Gern, J. F. Gundlach, A. Ko, A. Naghshineh-Pour, E. Sulaeman, P. -A. Tetrault, B. Grossman, R. K. Kapania, W. H. Mason and J. A. Schetz and R. T. Haftka, "Multidisciplinary Design Optimization of a Transonic Commercial Transport with a Strut-Braced Wing", 1999 World Aviation Conference, October 19-21, 1999, San Francisco, CA, AIAA-SAE paper 1999-01-5621

[4] A. Ko, B. Grossman, W.H. Mason and R. T. Haftka, "The Role of Constraints in the MDO of a Cantilever and Strut-Braced Wing Transonic Commercial Transport Aircraft", 2000 World Aviation Conference, October 10-12, 2000, San Diego, CA, AIAA-SAE paper 2000-01-5609

[5] J.F. Gundlach IV, P-A. Tétrault, F. Gern, A. Nagshineh-Pour, A. Ko, J.A. Schetz, W.H. Mason, R. Kapania, B. Grossman, R.T. Haftka, "Multidisciplinary Design Optimization of a Strut-Braced Wing Transonic Transport", AIAA 2000-0420, 38th Aerospace Sciences Meeting & Exhibit, 10-13 January 2000, Reno, Nevada

[6] Andy Ko, W.H. Mason and B. Grossman "Transonic Aerodynamics of a Wing/Pylon/Strut Juncture, AIAA-2003-4062, 21st AIAA Applied Aerodynamics Conference, 23-26 June 2003 / Orlando, FL

[7] Philippe-André Tétrault, "Numerical Prediction of the Interference Drag of a Streamlined Strut Intersecting a Surface in Transonic Flow", PhD Dissertation, Virginia Polytechnic Institute and State University, January 31, 2000

[8] Ohad Gur, Joseph A. Schetz, and William H. Mason, "Aerodynamic Considerations in the Design of Truss-Braced-Wing Aircraft", Journal of Aircraft, Vol. 48, No. 3, May–June 2011

[9] M. K. Bradley and C. K. Droney, "Subsonic Ultra Green Aircraft Research: Phase I Final Report", NASA/CR–2011-216847, April 2011.

[10] L. Cambier L. and J.-P. Veuillot, "Status of the elsA Software for Flow Simulation and Multi-Disciplinary Applications", 46th AIAA Aerospace Sciences Meeting and Exhibit, January 2008.

[11] R. Butler, W. Liu, Optimisation of stiffened panels using finite strip models, Buckling and

Postbuckling Structures, Imperial College Press, London, 2009, pp.225-257

[12] C. Kassapoglou, Design and analysis of composite structures with applications to aerospace structures, Wiley, 2010

[13] M.C. Niu, Composite Airframe Structures. Practical Design Information and Data on Aircraft Structures, Honk Kong Conmilit Press, 2006

[14] K.J. Bathe, Finite element procedures in engineering analysis, Prentice Hall, 1982

[15] MSC.Software Corporation, 'Aeroelastic Analysis – User's Guide', 2002.

[16] Albano E., Rodden W.P., 'A Doublet-Lattice Method for Calculating Lift Distributions on Oscillating Surfaces in Subsonic Flows', AIAA Journal, Vol. 7, issue 2, pp. 279-285, 1969.

[17] Dat R., Meurzec J-L., 'On the Flutter Calculations by the so-called "Reduced Frequency Scanning" Method', La Recherche Aérospatiale N° 133 pp. 41-44, 1969.

[18] Tran D.-M., Liauzun C., Labaste C., 'Method of Fluid-Structure Coupling in Frequency and Time Domains using Linearized Aerodynamics for Turbomachinery', Journal of Fluids and Structures 17, pp. 1161-1180, 2003.

[19] MIL_F-8785C, sec. 3.3.4 "Roll effectiveness"

[20] FAR 25.149(h)(3): "Minimum Control Speed"

[21] FAR 23.157(a)(2): "Rate of Roll".

Copyright Statement